Site preference of the M atom in $(Fe_{1-x}M_x)_3Ga$ (M identical to Cr, Mn, Co or Ni)

1989 J. Phys.: Condens. Matter 1 5115

(http://iopscience.iop.org/0953-8984/1/31/010)

J. Phys.: Condens. Matter **1** (1989) 5115–5123. Printed in the UK

Site preference of the M atom in $(Fe_{1-x}M_x)_3Ga$ $(M \equiv Cr, Mn, Co$ or $Ni)$

S Ishida†, S Fujii†, N Shinmura† and S Asano‡
† Department of Physics, Faculty of Science, Kagoshima University, Kagoshima 890, Japan
‡ Institute of Physics, College of Arts and Sciences, University of Tokyo, Meguroku, Tokyo 153, Japan

Received 14 June 1988, in final form 31 January 1989

Abstract. Energy band calculations were carried out for $(Fe_{1-x}M_x)_3Ga$ with $x = 0$ or $\frac{1}{12}$ to investigate the site preference of M atoms and the magnetic properties. It is shown that the site preference can be predicted from the total energy and is closely related to the density of states of two kinds of Fe in Fe_3Ga. Furthermore it is found that the magnetic moment on Cr or Mn in Fe_3Ga is antiparallel and on Co or Ni is parallel to the moment of Fe.

1. Introduction

There have been several experimental and theoretical investigations on Fe_3D (D ≡ Al, Si) with a $D0_3$ crystal structure. The $D0_3$ Fe_3D has two non-equivalent sites for Fe atoms. One, denoted by Fe_I, is surrounded by eight Fe atoms in an octahedral configuration and the other, denoted by Fe_{II}, is surrounded by four D atoms and four Fe atoms in a tetrahedral configuration.

Recently the structural and magnetic properties of $(Fe_{1-x}M_x)_3Ga$ (M ≡ Cr, Mn, Co or Ni) have been investigated by Kawamiya and Adachi (1983). They determined the structural and magnetic phase diagram of $(Fe_{1-x}M_x)_3Ga$ and showed that these systems form a $D0_3$ crystal structure over a wide x region, although Fe_3Ga forms an $L1_2$ crystal structure. Furthermore they found the preferential site occupation of the M atom in those systems; that is, Ni and Co enter the Fe_{II} sites, while Cr and Mn enter the Fe_I sites. The same site preference was found for transition-metal impurities in Fe_3Si (Burch *et al* 1981). Swintendick (1976) discussed the site preference of transition-metal impurities in Fe_3Si, making use of a rigid-level model based on his energy band calculation for paramagnetic Fe_3Si. Garba and Jacobs (1986) calculated electronic structures of Fe_3Si with various substitutional impurities on various sites from a tight-binding model. However, there is no self-consistent calculation of the energy band not only for impure Fe_3Si but also for pure or impure Fe_3Ga.

In this paper, we calculate the electronic structures not of only $D0_3$ Fe_3Ga but also of the systems $(Fe_{1-x}M_x)_3Ga$ (M ≡ Cr, Mn, Co or Ni) by the LMTO method and examine the magnetic properties and the relation between the electronic structures and the site preference of M atoms. For each system $(Fe_{1-x}M_x)_3Ga$ at a given x, we consider two

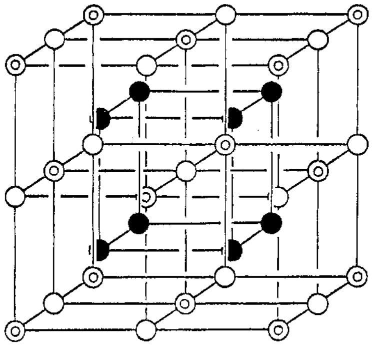

Figure 1. The primitive unit cell of Fe_3Ga: ◎ indicates Ga; ○, Fe_I; ●, Fe_{II}.

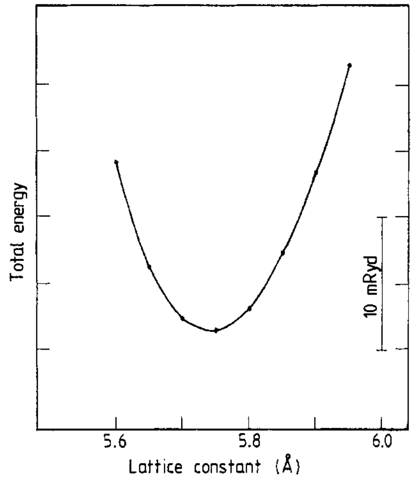

Figure 2. Total energies of paramagnetic Fe_3Ga for various lattice constants.

cases: M substitution into the Fe_I site and M substitution into the Fe_{II} site. Comparing the total energies of the two cases, we show which of two sites the M atom prefers.

2. Crystal structure and method

The crystal structure of $D0_3$ Fe_3Ga is shown in figure 1, which has a space group O_h^5 ($F_{m\bar{3}m}$). There are 16 atoms in the primitive unit cell: four Ga atoms in 4a sites, four Fe_I atoms in 4b sites and eight Fe_{II} atoms in 8c sites. For the systems $(Fe_{1-x}M_x)_3Ga$, we consider the case for $x = \frac{1}{12}$; that is, one M atom is substituted for one Fe atom in four molecules of Fe_3Ga. When the M atom occupies one Fe_I site, the structure has a space group O_h^1 ($P_{m\bar{3}m}$) and the atomic configuration in the primitive unit cell is as follows; one M in 1b, one Ga in 1a, three Ga in 3c, three Fe_I in 3d and eight Fe_{II} in 8g. The positional parameter of the 8g site is $\frac{1}{2}$. On the contrary, when the M atom occupies one Fe_{II} site, the structure has a space group T_d^1 ($P_{\bar{4}3m}$) and the configuration is as follows: one M in 1b, one Fe_{II} in 1a, three Fe_{II} in 3c, three Fe_{II} in 3d, four Ga in 4e and four Fe_I in 4e. The positional parameters of the 4e site are $\frac{3}{2}$ for Ga and $\frac{1}{2}$ for Fe_I. Local atomic configurations in $(Fe_{1-x}M_x)_3Ga$ are listed in table 1.

Band calculations were carried out self-consistently by the LMTO method (Andersen *et al* 1985). The exchange–correlation potentials were treated within the framework of the local-spin-density (LSD) approximation (Moruzzi *et al* 1978). Crystal potentials were assumed to be spherical in the Wigner–Seitz (WS) sphere (WS radii are the same for all constituent atoms). The maximum angular momenta l_{max} describing the wavefunctions were chosen as $l_{max} = 2$ for all atoms. The self-consistency was achieved at 85 or 19 k-points in the irreducible Brillouin zone for paramagnetic or ferromagnetic $D0_3$ Fe_3Ga. For $(Fe_{1-x}M_x)_3Ga$, it was achieved at 20 k-points for M ≡ Co or Ni and at 35 k-points for for M ≡ Ni or Cr because the convergence against k-points is worse for the latter than for the former. The self-consistent iterations were carried out for both core and valence states. The density of states (DOS) was obtained by the tetrahedral integration method (Rath and Freeman 1975).

Table 1. Local atomic configurations in $(Fe_{1-x}M_x)_3Ga$ at $x = \frac{1}{12}$. The figures in parentheses show positions of atoms in the unit cell and those before elements show numbers of neighbouring atoms.

M atom in Fe_I sites	1st neighbours	2nd neighbours
M	$8Fe_{II}$	6Ga(3c)
Fe_I	$8Fe_{II}$	2Ga(1a), 4Ga(3c)
Fe_{II}	1M, 1Ga(1a), 3Ga(3c), $3Fe_I$	$6Fe_I$
M atom in Fe_{II} sites	**1st neighbours**	**2nd neighbours**
M	4Ga, $4Fe_I$	$6Fe_{II}$(3c)
Fe_I	1M, $1Fe_{II}$(1a), $3Fe_{II}$(3c), $3Fe_{II}$(3d)	6Ga
Fe_{II}(1a)	4Ga, $4Fe_I$	$6Fe_{II}$(3d)
Fe_{II}(3c)	4Ga, $4Fe_I$	2M, $4Fe_{II}$(3d)
Fe_{II}(3d)	4Ga, $4Fe_I$	$2Fe_{II}$(1a), $4Fe_{II}$(3c)

For the systems $(Fe_{1-x}M_x)_3Ga$ (M ≡ Cr or Mn), we assumed at first in the self-consistent iteration that the magnetic moments of Cr and Mn are antiparallel to those of Fe atoms, because the measured values of the saturation magnetic moment of the systems are smaller than those estimated from a simple dilution (Kawamiya and Adachi 1983). The initial values of magnetic moments are as follows: $-1.5\,\mu_B$, $-1.0\,\mu_B$, $2.5\,\mu_B$, $1.8\,\mu_B$, $0.5\,\mu_B$, $0.4\,\mu_B$ and 0 for Cr, Mn, Fe_I, Fe_{II}, Co, Ni and Ga, respectively.

3. Results and discussions

First we calculated the total energy of paramagnetic $D0_3$ Fe_3Ga for various lattice constants and obtained the result that the total energy possesses a minimum for the value of 5.743 Å (figure 2). This value is a little smaller than the experimental value (Kawamiya *et al* 1972). However, we used the value of 5.743 Å for the lattice constants of ferromagnetic $D0_3$ Fe_3Ga and the systems $(Fe_{1-x}M_x)_3Ga$ (M ≡ Cr, Mn, Co or Ni).

The DOS curves of iron d bands for paramagnetic Fe_3Ga are shown in figure 3. As could be guessed from the atomic configuration, the DOS of Fe_I is similar to that of pure iron d bands and has a two-peak structure which is characteristic of BCC Fe. Between these peaks, there exists a deep valley. The DOS of Fe_{II} has a more complex structure than that of Fe_I and peaks at the deep valley of the DOS of Fe_I. Since the peak of Fe_I is higher than that of Fe_{II} near the Fermi level, it is expected that the magnetic moment of Fe_I is larger than that of Fe_{II} in a ferromagnetic state.

The DOS curves of iron d bands in ferromagnetic Fe_3Ga are shown in figure 4. It is seen that up-spin states are almost occupied in both Fe_I and Fe_{II} and that the down-spin states are unoccupied much more for Fe_I than for Fe_{II}. The calculated values of the magnetic moment are $-0.10\,\mu_B$, $2.38\,\mu_B$ and $2.09\,\mu_B$ for Ga, Fe_I and Fe_{II}, respectively. The experimental values obtained by neutron diffraction are (2.2–2.5 μ_B) for Fe_I and less than 1.7 μ_B for Fe_{II} (Kawamiya and Adachi 1982). The calculated value for Fe_{II} is somewhat larger than the experimental value.

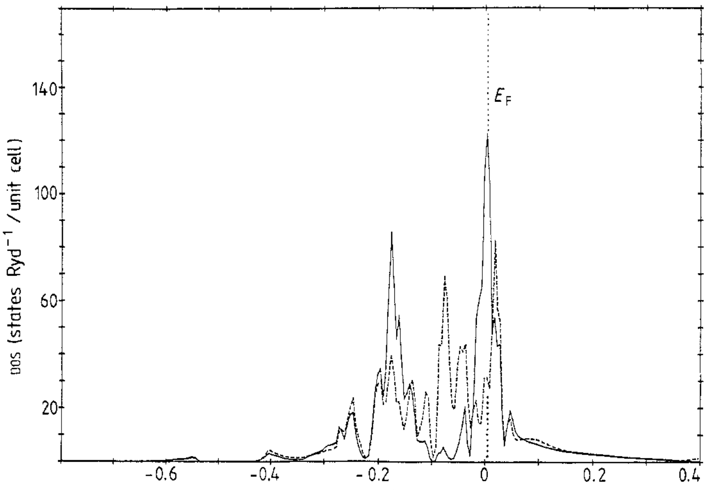

Figure 3. The DOS curves of iron d bands in paramagnetic Fe_3Ga. The solid and broken curves show the DOS of Fe_I and Fe_{II} respectively. The Fermi level is indicated by the vertical dotted line.

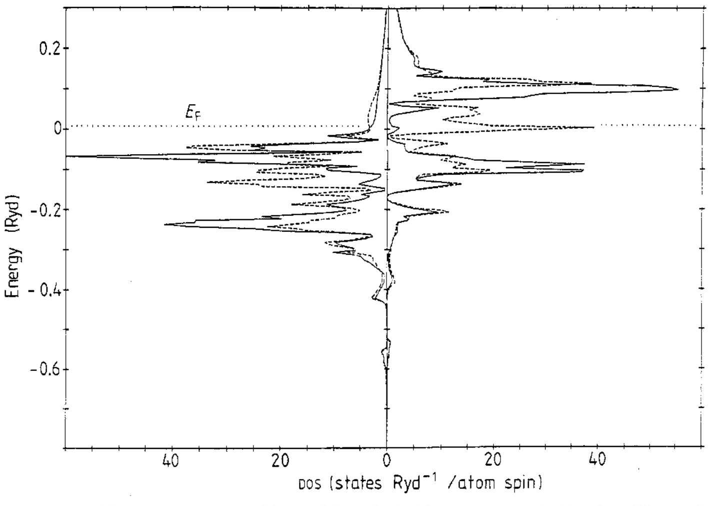

Figure 4. The DOS curves of iron d bands in Ferromagnetic Fe_3Ga. The solid and broken curves show the DOS of Fe_I and Fe_{II} respectively. The DOS curves for up-spin electrons are shown on the left and those for down-spin on the right. The Fermi level is indicated by the horizontal dotted line.

The numbers of electrons in WS spheres are listed in table 2 for constituent atoms of Fe_3Ga. The difference between the number of electrons of an atom in Fe_3Ga and that of the free atom are also given, together with the numbers of electrons for each angular momentum. From this table, we notice that electrons transfer from Ga atoms to Fe atoms and that the number n_t of transferred electrons is larger for Fe_{II} than for Fe_I; in other words, Fe_I and Fe_{II} are electronegative and Fe_{II} is more electronegative than Fe_I.

Table 2. Numbers of valence electrons with angular momentum l in the WS sphere and numbers of transferred electrons n_t.

		s	p	d	Sum	n_t
Fe_I	Major	0.311	0.379	4.539	5.230	0.084
	Minor	0.329	0.428	2.097	2.854	
Fe_{II}	Major	0.291	0.387	4.427	5.105	0.117
	Minor	0.292	0.429	2.290	3.012	
Ga	Major	0.528	0.710	5.052	6.290	−0.317
	Minor	0.537	0.814	5.041	6.393	

Thus, it may be said that an element electronegative to Fe prefers Fe_{II} sites, as indicated by Swintendick (1976) for Fe_I and Fe_{II} sites in Fe_3Si.

For $(Fe_{1-x}M_x)_3Ga$ at $x = \frac{1}{12}$ (M ≡ Cr, Mn, Co or Ni), as already mentioned, we consider two cases: type I, M substitution into the Fe_I site; type II, M substitution into Fe_{II}. Figure 5 shows the partial DOS curves of M and Fe atoms for type I and figure 6 shows those for type II. Although there are three different sites for Fe_{II} atoms in the unit cell of the type II, we show only the DOS of Fe_{II} in 3d sites because the DOSs of Fe_{II} in different sites are quite similar to each other. From the figures, we note that the DOS of Fe_I (Fe_{II}) in $(Fe_{1-x}M_x)_3Ga$ has the structure of the DOS of Fe_I (Fe_{II}) in Fe_3Ga. For both types, the band width of M atoms becomes narrow and the DOS shifts to an increasingly lower energy in the order Cr, Mn, Co, Ni, since the potential around M atoms becomes increasingly deeper in that order. Paying attention to the DOS of M atoms in figure 5, we note that the DOS has the same two-peak structure as Fe_I although the peak in the lower-energy region is low for up-spin states of Cr and Mn and the detailed structure of the main peaks is changed from that of Fe_I owing to the hybridisation between d bands of M and Fe atoms. On the contrary, the DOS of M atoms of type II in figure 6 is similar to that of Fe_{II} except for that of Cr and Mn for up-spin states. From these figures, we can also see that the up-spin bands are more occupied than the down-spin bands for Fe_I, Fe_{II}, Co and Ni in both types, but the down-spin bands are more occupied for Cr and Mn. That is, the magnetic moments on Cr and Mn are antiparallel to those of Fe, while those of Co and Ni are parallel.

The calculated magnetic moments on the constituent atoms in $(Fe_{1-x}M_x)_3Ga$ are given in table 3, together with saturation moments per formula unit (Kawamiya and Adachi 1983). We note that the moments on Fe do not differ much from those on the corresponding Fe in Fe_3Ga except for Fe_{II} in type I, where the moment on Fe_{II} is almost equal to that on Fe_{II} in Fe_3Ga for the case of M ≡ Co or Ni but is about 0.5 μ_B smaller for M ≡ Cr or Mn. This is considered to be due to the difference of neighbours; as seen in table 1, Fe_{II} has one M atom in the first neighbours for type I but does not for type II. Paying attention to the DOS of Fe_{II} in type I, it is found that the unoccupied DOS of the up-spin states is larger for M ≡ Cr or Mn than for M ≡ Co or Ni since above the Fermi level the hybridisation between the d bands of M and Fe_{II} is stronger for M ≡ Cr or Mn. This causes a decrease in the magnetic moment on Fe_{II} for M ≡ Cr or Mn. Experimental results (Kawamiya and Adachi 1983) show that the saturation magnetic moment of the real system for M ≡ Cr or Mn is smaller than that estimated from a simple dilution. The moment reduction is attributable to the moment decrease of Fe_{II} and to antiparallel moments on Cr or Mn.

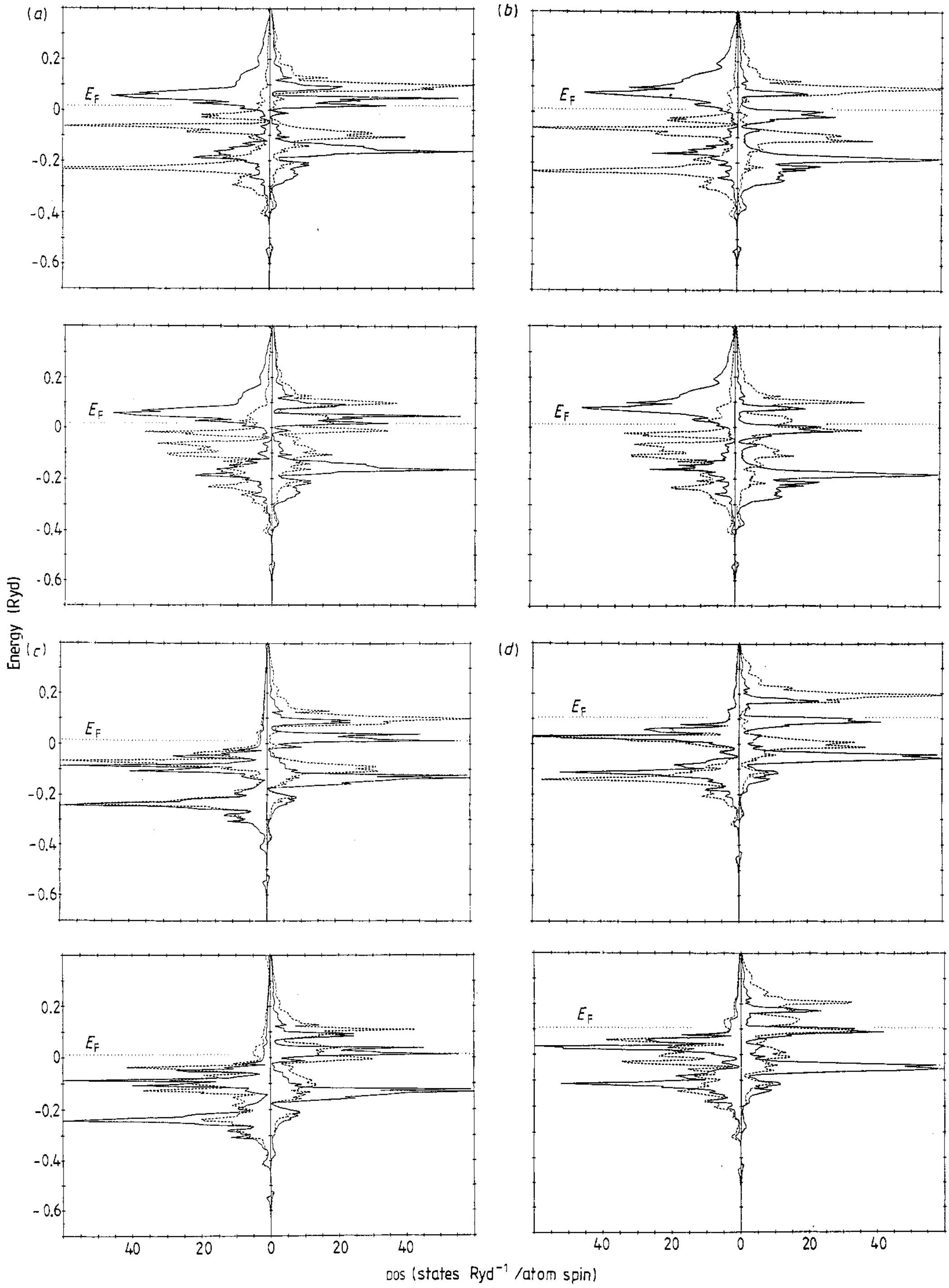

Figure 5. The DOS curves of d bands of constituent atoms in $(Fe_{1-x}M_x)_3Ga$ for the case of type I: (*a*) M ≡ Cr; (*b*) M ≡ Mn; (*c*) M ≡ Co; and (*d*) M ≡ Ni. For each part, the DOS of M and Fe_I are shown on top with those of M and Fe_{II} below. In each figure, the solid and broken curves show the DOS of M and Fe atoms respectively and the DOS curves for up-spin electrons are shown on the left, and those for down-spin on the right.

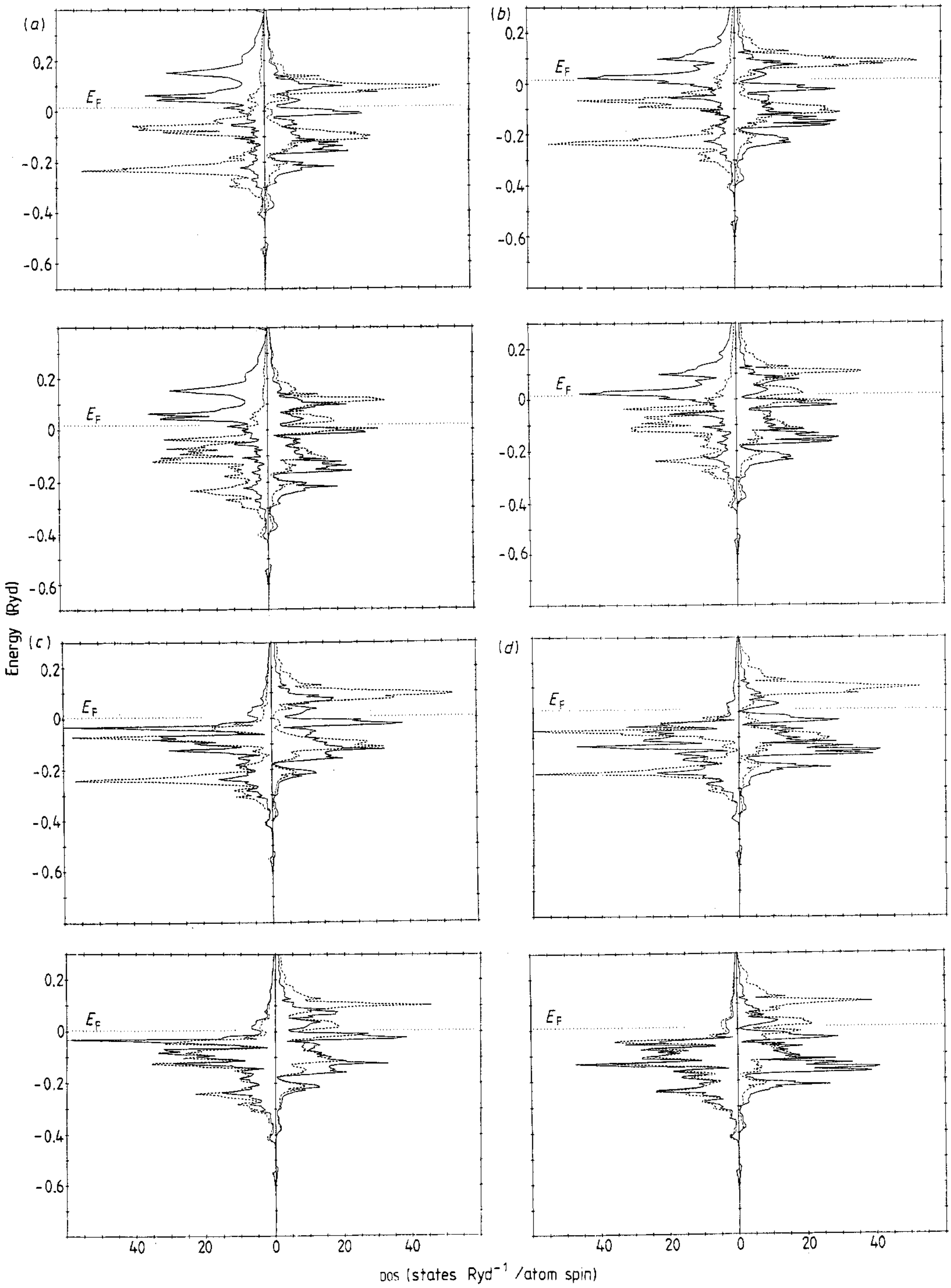

Figure 6. The DOS curves of d bands of constituent atoms in $(Fe_{1-x}M_x)_3Ga$ for the case of type II: (*a*) M ≡ Cr, (*b*) M ≡ Mn, (*c*) M ≡ Co and (*d*) M ≡ Ni. For each part, the DOS of M and Fe_I are shown on top, with those of M and Fe_{II} below. In each figure, the solid and broken curves show the DOS of M and Fe atoms respectively and the DOS curves for up-spin electrons are shown on the left and those for down-spin on the right.

Table 3. Magnetic moments of atoms in $(Fe_{1-x}M_x)_3Ga$ (M≡Cr, Mn, Co and Ni). The unit is μ_B. The sites of atoms are given in parentheses.

	Type I (M in Fe_I sites)						
	M(1b)	Ga(1a)	Ga(3c)	Fe_I(3d)	Fe_{II}(8d)	FU	Exp.
Cr	−1.17	−0.10	−0.07	2.51	1.53	4.58	4.93
Mn	−2.98	−0.12	−0.08	2.49	1.63	4.29	5.00
Co	1.64	−0.10	−0.09	2.44	1.97	6.09	
Ni	0.41	−0.10	−0.10	2.42	2.01	5.83	

	Type II (M in Fe_{II} sites)							
	M(1b)	Ga(4e)	Fe_I(4e)	Fe_{II}(1a)	Fe_{II}(3c)	Fe_{II}(3d)	FU	Exp.
Cr	−2.02	−0.07	2.32	2.21	1.90	2.03	5.24	
Mn	−1.71	−0.07	2.37	2.04	1.86	2.01	5.29	
Co	0.68	−0.09	2.50	1.99	1.87	2.00	5.98	5.65
Ni	0.40	−0.09	2.51	2.12	2.07	2.14	6.20	5.55

The differences between the total energies of type I and type II are 0.012 Ryd FU^{-1}, −0.004 Ryd FU^{-1}, −0.034 Ryd FU^{-1} and −0.053 Ryd FU^{-1} for M ≡ Cr, Mn, Co and Ni, respectively. These results indicate that Cr impurities energetically prefer Fe_I sites, while Mn, Co and Ni impurities prefer Fe_{II} sites. However, we cannot predict with certainty the site preference of Mn considering the accuracy of our calculation because the difference between total energies is very small. Apart from Mn, our results are consistent with the experimental results. Next we consider the relationship between the site preference and the DOS obtained.

We consider only the contribution of d electrons of M atoms to the total energy which may be most important to discuss the site preference. Comparing the DOS of Cr in figure 5(*a*) with that in figure 6(*a*), we note that the DOS in the lower-energy region is higher in figure 5(*a*) than in figure 6(*a*). Therefore the d electrons of Cr favour the d bands of type I rather than those of type II. For Mn, the same situation is seen on comparing the DOS of Mn in figure 5(*b*) with that in figure 6(*b*). On the contrary, for Ni there are peaks in figure 6(*d*) between the two main peaks in figure 5(*d*). The d electrons of Ni favour the d bands of type II owing to the central peaks since these peaks supplement the energy loss due to the low DOS in the lower-energy region with the energy gain due to the DOS in the higher-energy region. For Co, the same situation is seen but the effect of the central peaks is weaker since the DOS of the central peaks are smaller than those for Ni.

These features, as described above, are roughly explained as follows on the basis of the rigid-band model using the DOS of Fe_I and Fe_{II} in Fe_3Ga. When the number of d electrons of M atoms such as Cr is low, the d electrons tend to occupy the d bands of Fe_I rather than those of Fe_{II} because of the high DOS in the lower-energy region. On the contrary, when the number of d electrons of M atoms such as Ni is high, the d electrons tend to occupy the d bands of Fe_{II} because of the high DOS in the central-energy region of the d bands. That is, M atoms prefer the Fe_I sites when the number of d electrons is low but the Fe_{II} sites when the number is high. This conjecture is consistent with our results of the total energy of the systems. Thus the difference between the DOSs of Fe_I

and Fe_{II} in Fe_3Ga is an important factor to consider in the site preference of M atoms in $(Fe_{1-x}M_x)_3Ga$.

We performed another calculation for type I of the case M ≡ Cr using the same initial condition except that the initial moment on Cr is parallel to that on Fe. The total energy of this case is a little higher than the case of the anti-parallel moment on Cr. The moments obtained do not differ much from those given in table 3 except for Cr and Fe_{II} ($-0.56\ \mu_B$ for Cr and $1.64\ \mu_B$ for Fe_{II}). Although we assumed that the initial moment on Cr was parallel to that on Fe, the moment on Cr obtained finally in the self-consistent iteration is anti-parallel to that on Fe. Thus we can guess that the antiferromagnetic coupling between the moments of Cr and Fe is very strong. However, we cannot explain only from our calculations why Cr and Mn couple antiferromagnetically to the surrounding Fe.

As described above, we have considered two types of ordered alloy in order to investigate the site preference of M atoms in $(Fe_{1-x}M_x)_3Ga$: they have M atoms substituted for Fe_I or Fe_{II}, respectively. We obtained the correct site preference of M atoms in the systems $(Fe_{1-x}M_x)_3Ga$ (M ≡ Cr, Mn, Co or Ni) except for Mn from total-energy differences and showed that our conjecture about the relationship between the site preference and the difference between the DOSs of Fe_I and Fe_{II} in Fe_3Ga is not inconsistent with the experimental results. Furthermore we obtained the result that the moment reduction in the real system (M ≡ Cr or Mn) is attributable to the moment decrease of Fe_{II} atoms and to the antiparallel moments of Cr and Mn atoms. We have considered only the M concentration x of $\frac{1}{12}$; therefore, our calculation is not extensive enough to discuss the site preference for the whole composition range. However, our results must be helpful in discussing the site preference and magnetic properties for alloys of the type Fe_3D (D ≡ Al, Si, etc).

Acknowledgments

We would like to thank Professor K Adachi of Nagoya University and Professor N Kawamiya of Chukyo University for providing us with information. This work was partially supported by the Grant-in-Aid for Scientific Research from the Ministry of Education of Japan. The numerical calculations were performed on a FACOM M-780 at the Computer Center of Kyushu University and a HITAC M-280H at the Computer Center of the University of Tokyo.

References

Andersen O K, Jepsen O and Glotzel D 1985 *Proc. Int. School of Physics 'Enrico Fermi', Course* **89** 59
Burch T J, Budnick J I, Niculescu V A, Raj K and Litrenta T 1981 *Phys. Rev.* B **24** 3866
Garba E J D and Jacobs R L 1986 *J. Phys. F: Met. Phys.* **16** 1485
Kawamiya N and Adachi K 1982 *Trans. Japan Inst. Metall.* **23** 296
—— 1983 *J. Magn. Magn. Mater.* **31–4** 145
Kawamiya N, Adachi K and Nakamura Y 1972 *J. Phys. Soc. Japan* **33** 1318
Moruzzi V L, Janak J F and Williams A R 1978 *Calculated Electronic Properties of Metals* (New York: Pergamon)
Rath J and Freeman A J 1975 *Phys. Rev.* B **11** 2109
Swintendick A C 1976 *Solid State Commun.* **19** 511